


Research Article

Effect of Abrasive Concentration on Impact Performance of Abrasive Water Jet Crushing Concrete

Xiaohui Liu ^{1,2}, Ping Tang,³ Qi Geng,¹ and Xuebin Wang¹

¹Key Laboratory of Road Construction Technology and Equipment of MOE, School of Construction Machinery, Chang'an University, Xi'an 710064, China

²Post-Doctoral Research Center, Sinomach Changlin Company Limited, Changzhou 213136, China

³Xi'an Automotive Technology Vocational College, Xi'an 710038, China

Correspondence should be addressed to Xiaohui Liu; chd160039@chd.edu.cn

Received 13 November 2018; Accepted 4 February 2019; Published 6 March 2019

Academic Editor: Francesco S. Marulo

Copyright © 2019 Xiaohui Liu et al. This is an open access article distributed under the Creative Commons Attribution License, which permits unrestricted use, distribution, and reproduction in any medium, provided the original work is properly cited.

It has been found that the impact performance of water jets can be changed by its properties, which include pressure, additive, and mode of jet. Thus, an abrasive water jet (AWJ) has been developed as a new method. However, there is little research on the effect of abrasive concentration on the impact performance of abrasive jets. Thus, the SPH method is used to establish an abrasive water jet crushing concrete model to study the effect of abrasive concentration on the impact force, concrete internal energy, abrasive particle distribution, crushing depth, and damage and crushing efficiencies under different concrete compressive strengths and abrasive densities. The results indicate that there is little effect of the abrasive concentration on the peak impact force under different compressive strengths and abrasive densities, while the mean impact force tends to increase linearly with the abrasive concentration. The internal energy of the concrete increases stepwise with the abrasive concentration under different compressive strengths and abrasive densities. The concentration of 10%~20% is the rapid increasing stage. The crushing depth and damage efficiencies are all maximum at a concentration of 20% under different compressive strengths and abrasive densities. After the concrete was impacted by the water from the water jet, it is divided into rebounding particles and intrusive particles. The more the intrusive particles, the easier the concrete to be crushed and damaged.

1. Introduction

Water jet technology has been widely applied in machinery, civil construction, gas drainage, and cleaning operations, especially in mining and petroleum drilling [1]. Concrete breaking by using tools is assisted by water jets to not only decrease the contact between cutting tools and concrete but also increase the free surface around the concrete impact by using tools for superior breakage.

On the one hand, much research has focused on the impact performance of pure water jets. Material cutting by a pure water jet is shown in Figure 1(a). Ozcelik et al. [2, 3] focused on the stone surface treatment with water jets and concluded that the application of water jets in surface treatment enabled obtaining a surface with required roughness while preserving aesthetic appearance of the stone. Dehkhoda and Hood [4, 5] observed the capacity of

pulsed water jets for creating an internal breakdown and the relative contributions of the pulse length and pulsation frequency on the surface and subsurface damage caused by a pulsed water jet on rock targets.

On the other hand, the assisting performance of water jets in rock breaking by using tools was also studied. Tools cutting the material assisted by the water jet are shown in Figures 1(b)–1(d), which include a disc cutter, drill bit, and conical tool. Ciccu and Grosso [7] dealt with the problems of assisting disc cutters with high-velocity water jets to increase the excavation rate and to improve the working conditions, with particular reference to wear. Yang et al. [6] studied the wear characteristics of cemented carbide blades in drilling limestone with a water jet, concluding that the wear rate decreases with the nozzle diameter in the drill bit. Ciccu and Grosso [8] carried out the experimental research aimed both at studying the processes by which mechanical excavation is

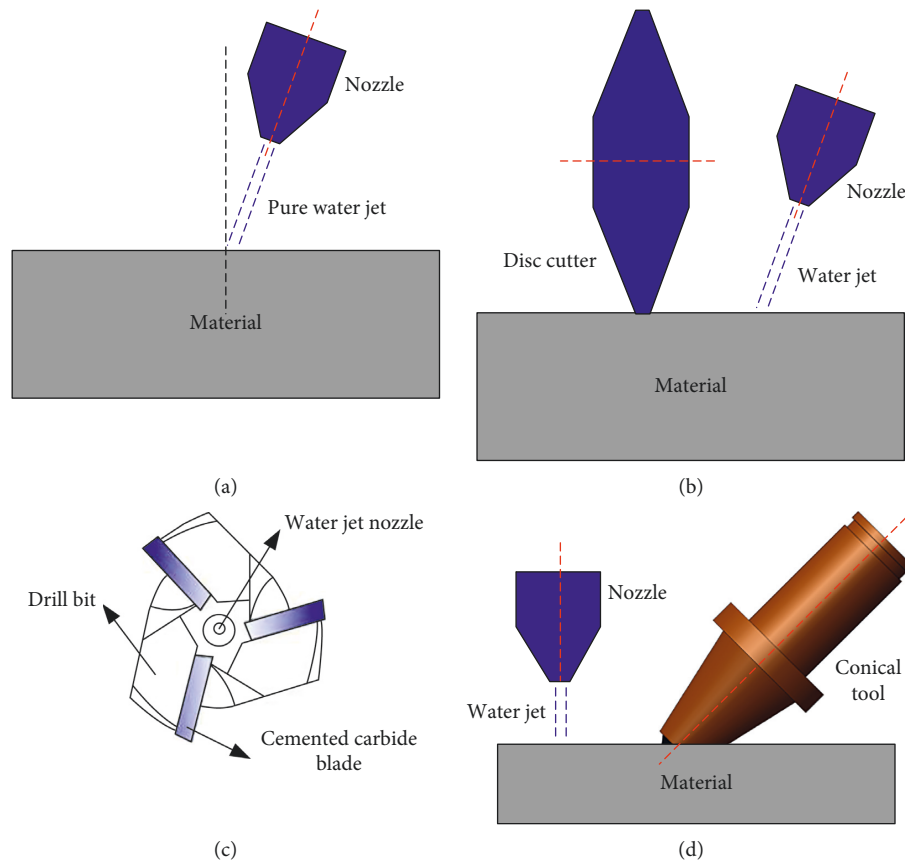


FIGURE 1: (a) Pure water jet. Disc tool (b), drill bit [6] (c), and conical tool (d) assisted by water jets.

improved and at quantifying the increment of the excavation performance parameters with water jets. In that paper, the water jet was directed in front of the tool. Liu et al. [9–13] performed numerical simulations and experiments to study the rock breaking performance of different configuration modes of conical tools assisted by water jets.

After a long period of research, researchers have found that the impact performance of water jets can be changed by changing their properties. The properties of water jets include pressure, additive (abrasive jet), and mode of jet (pulsed jet). Thus, with the development of water jet technique, an abrasive water jet (AWJ) assistance, as a new method, has been developed in hard rock mechanical cutting and drilling [14]. Selvam et al. [15] observed abrasive water jet machining of composite laminates experimentally for various cutting parameters in terms of average surface roughness and kerf taper. By generating a response surface model, the experimental values obtained for quality characteristics were empirically related to those of cutting parameters. Wong et al. [16] pointed out that kerf taper and delamination were undesirable geometrical defects inherent to abrasive water jet machining (AWJM) of layered fibre-reinforced polymer composites and described an experimental investigation in minimizing the defects for hybrid fibre-reinforced polymer composites.

All the above researchers conducted studies on abrasive water jets experimentally. Actually, it is difficult to research the fracture mechanism of target material crushing by using

abrasive water jets in experiments because of high speed and high pressure of water jets and opaqueness of most target materials. And a water jet crushing a target material is a process of nonlinear impact dynamics, which contains many problems in short time, such as fluid-solid coupling, high strain rate, and large deformation. As a very important method in current scientific research, simulation technology has the advantages of high reliability and low economic cost. Domestic and foreign researchers have used this technology to conduct many numerical simulations on the process of abrasive water jet cutting and crushing materials.

For the simulation of abrasive water jet crushing materials, different scholars use different methods. Scholars usually use CFD methods for research when focusing on flow field problems of abrasive jets. Liu et al. [17, 18] studied the flow field characteristics of the abrasive water jet by using the CFD method. The CFD model was established based on three-phase (air, water, and particle) turbulent flow. Plausible characteristics of the flow as well as the particle velocity and trajectory under different input conditions were predicted and discussed. The powerful computational fluid dynamics (CFD) analysis software Fluent was applied to numerical simulation of liquid-solid two-phase flow in the hard alloy nozzle of different cylindrical section lengths under a certain condition [19]. Meng et al. [20] used Fluent software to get the isothermal, incompressible, steady flow field out of a submerged abrasive water jet nozzle through numerical simulation, with different particle sizes and different confining

pressures under submerged conditions. Deepak et al. [21] carried out the jet flow through the AWJ nozzle with different nozzle geometries using computational analysis.

These studies provide a viable method for fluid-solid coupling simulation of water and abrasives in abrasive jets. However, this method cannot simulate the cutting process of abrasive jets. That is to say, the target material cannot be included in the established simulation model, and the impact performance of the abrasive jet cannot be studied.

In the simulation of abrasive jet cutting materials, the target material is usually established using the Lagrangian finite element method (FEM). To make the established abrasive jet model both couple with the material model and simulate the large deformation characteristics of water, the ALE method is used to establish the water, abrasive, and air models. Gong et al. [22] used LS-DYNA to simulate the abrasive water jet crushing materials and analyzed the effect of moving speed and pressure on cutting depth and erosion. Shahverdi et al. [23] used LS-DYNA to numerically simulate the abrasive water jet crushing low carbon steel alloy by using the ALE method.

Although the ALE method can effectively simulate abrasive jets, it still cannot fully simulate the actual crushing process. For example, the splash process after water impacted the material and the discrete properties of the abrasive particles cannot be simulated. To this end, researchers have begun to use the smooth particle hydrodynamics (SPH) method to simulate abrasive jets. Liu et al. [1] and Jiang et al. [24] used the SPH method to establish a pure continuous water jet and a discontinuous jet to study the performance of water jet cutting rock, respectively. Feng et al. [25] adopted the SPH-coupled FEM, in which SPH particles were used to model the high-speed water jet to adapt their extremely large deformation and FEM was applied to model the discrete abrasive particle, cutting head, and workpiece. However, only the acceleration process of a single abrasive particle was studied using this method. Compared with this method, Wang et al. [26] and Guo et al. [27] used SPH to model the abrasive and water at the same time, realized the random distribution of abrasive particles in water by a random algorithm, and studied the cutting performance of the abrasive jet cutting steel.

The above SPH method can effectively simulate water jets or even abrasive jets cutting and impacting materials, but there are still some shortcomings. First, there is little research on the effect of abrasive concentration on the impact performance of abrasive jets. And the range of abrasive concentrations studied is not comprehensive enough. For instance, Xue et al. [28] compared only the depth of concentrations of 6% and 12% of the abrasive jet impacting coal. Li et al. [29] performed simulation analysis and experimental study on the effect of different abrasive concentrations (2%, 4%, 6%, and 8%) on the quality of abrasive flow. Mu and Rong [30] studied the effect of the abrasive concentration, and the concentration was expressed by the amount of abrasive (1 particle, 2 particles, and 3 particles). Second, for the study of the SPH method, most scholars have neglected the study of the interaction and distribution between water and abrasive particles after crushing. Therefore, in this paper, the SPH method was used to establish the abrasive

water jet crushing concrete model to study the effect of abrasive concentration on the impact force, concrete internal energy, abrasive particle distribution, crushing depth, and damage and crushing efficiencies under different concrete compressive strengths and abrasive densities.

2. Methodology

In this paper, the computer program LS-DYNA, finite element software for simulation of geomaterials, was used. The numerical model for concrete crushing by using the abrasive water jet is shown in Figure 2.

The water jet and abrasive were first established by a set of SPH particles. Then, by extracting the series of SPH particle numbers, the established SPH particles were divided into a water particle group and an abrasive particle group according to the ratio of the abrasive to the water, and the abrasive particle group was randomly distributed in the water particle group, as shown in Figure 2. The set of SPH particles is shown in box, and the length is 12 mm. The width of the water jet is 1.2 mm. The velocity of the water jet is 280 m/s. Different abrasive concentrations of 5%, 10%, 20%, and 30% and different abrasive densities of 2000 kg/m³, 3000 kg/m³, 4000 kg/m³, and 5000 kg/m³ were set.

If the coordinate of a particle was x_i at initial time, it would be x_j at t time. Thus, the position of this particle was a function of the initial coordinate x_i , namely, $x_j = x_j(x_i, t)$. In hydromechanics, the following equations were often used to describe the motion and status of the fluid when the hydrodynamics problems were solved by using the SPH method [1, 25–27].

Position equation of the particle is

$$\frac{dx_i}{dt} = v_i. \quad (1)$$

Mass conservation equation of the particle is

$$\frac{d\rho_i}{dt} = \sum_{j=1}^N m_j (v_j - v_i) \cdot \nabla_i W_{ij}. \quad (2)$$

Momentum conservation equation of the particle is

$$\frac{dv_i}{dt} = \left[\frac{\sigma_j^{\alpha\beta}}{\rho_i^2} - \frac{\sigma_i^{\alpha\beta}}{\rho_j^2} \right] \cdot W_{ij,\beta}. \quad (3)$$

Energy conservation equation of the particle is

$$\frac{dE_i}{dt} = \sum_{j=1}^N m_j (v_j - v_i) \cdot \left[\frac{\sigma_j^{\alpha\beta}}{\rho_i^2} + \frac{1}{2} \Pi_{ij} \right] \cdot W_{ij,\beta} + H_i, \quad (4)$$

where ρ_i is the density of particle i , m_j is the mass of the particle j (kg), $\sigma_{\alpha\beta}$ is the stress tensor (Pa), v_i is the velocity of particle i (m/s), E_i is the energy per unit mass of particle i (J), Π is the artificial viscosity force (N), H is the artificial heat flux (J/s), and W is the kernel function of the particle.

The water jet was described by using the MAT_NULL and the GRUNEISEN equation of state (EOS) for pressure response. Its density was 1000 kg/m³, the dynamic viscosity was 0.001 Pa·s, and Poisson's ratio was 0.5 [1, 27]. The abrasive was also described by using the MAT-NULL model.

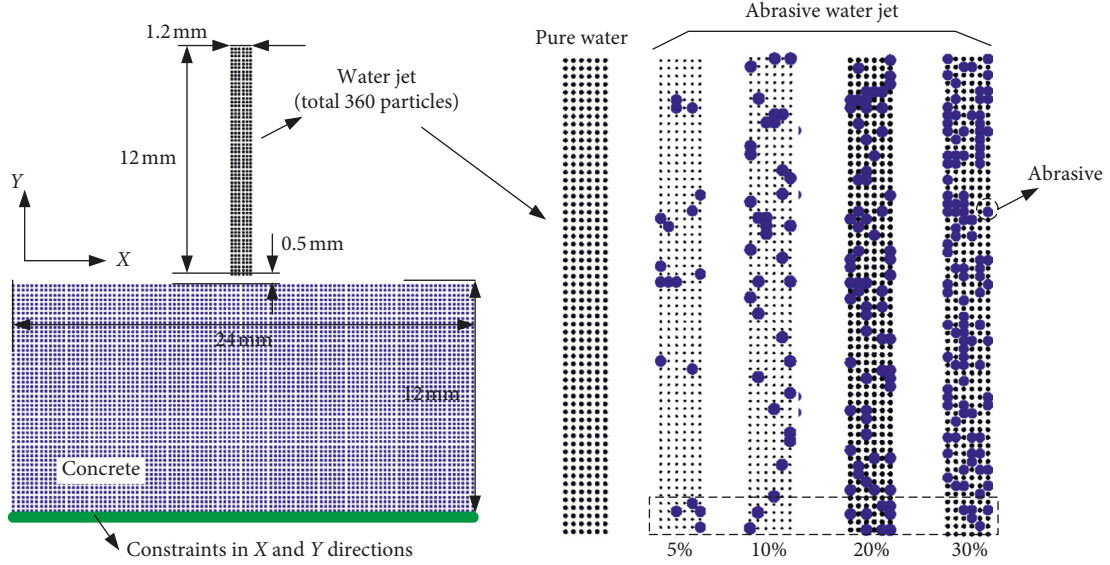


FIGURE 2: Numerical model for concrete crushing by the abrasive water jet.

The EOS_GRUNEISEN is given by the following equation to describe its pressure and volumetric strain relation:

$$Q = \frac{\rho c^2 \mu [1 + (1 - (\gamma_0/2))\mu - (\alpha/2)\mu^2]}{[1 - (S_1 - 1)\mu - S_2(\mu^2/\mu + 1) - S_3(\mu^3/(\mu + 1)^2)]^2} + (\gamma_0 + \alpha\mu)E, \quad (5)$$

where c is the intercept of the curve $\mu_s - \mu_p$, E is the internal energy of unit volume (J), S_i is the slope of the curve $\mu_s - \mu_p$, γ_0 is the EOS_GRUNEISEN coefficient, and α_0 is the correction coefficient about the relationship between γ_0 and volume.

The model of concrete was also established by using the SPH method. The concrete was 12×24 mm in dimension. X and Y direction displacement constraints were applied to the bottom of concrete. To simulate the strain and stress of concrete impacted by the abrasive water jet effectively, the material Johnson-Holmquist concrete was adopted to describe concrete material. The constitutive model has been used widely for simulating concrete subjected to large strains, high strain rates, and high pressures. Different concrete strengths of 20 MPa, 40 MPa, 60 MPa, and 80 MPa were set. The parameters are given in Table 1.

To determine the accuracy of the material model, the compressive strength and tensile strength of the concrete material were tested. The test model and results are shown in Figure 3. The concrete is 50×100 mm in dimension. A displacement constraint in the Y direction is applied to the bottom of the concrete, and a Y displacement load is applied to the top. According to repeated tests, the load rate has little effect on the concrete strength results. The test results show that the compressive strengths of the four materials are 20 MPa, 40 MPa, 60 MPa, and 80 MPa, and the tensile strengths are about 4 MPa, 4 MPa, 5 MPa, and 6 MPa, which basically satisfy that the tensile strength is about 1/20~1/10 of compressive strength for concrete. Therefore, the model parameters can be used to simulate concrete from 20 MPa to 80 MPa.

TABLE 1: Mechanical parameters of concrete.

Parameters	20 MPa	40 MPa	60 MPa	80 MPa
A_0			0.28	
B_0	1.20	1.24	1.28	1.32
N_0			0.84	
S_{\max}			15.0	
C_0			0.006	
ρ_0 (kg/m ³)			2410	
G (Pa)			5.8e9	
f'_c (Pa)	2.0e7	4.0e7	6.0e7	8.0e7
T (Pa)			1.0e6	
D_1			0.04	
D_2			1.0	
E_{\min}			0.01	
P_t (Pa)			1.6e7	
μ_t			0.001	
P_1 (Pa)			1.21e9	
μ_1			0.1	
K_1 (Pa)			1.2e10	
K_2 (Pa)			1.35e10	
K_3 (Pa)			6.89e10	

3. Results and Discussion

3.1. Effect of Abrasive Concentration under Different Compressive Strengths. To study the effect of abrasive concentrations on impact performance of the abrasive water jet under different compressive strengths, the abrasive concentrations were 5%, 10%, 20%, and 30% according to the existing literature that abrasive concentration ranged from 3% to 30%; the concrete compressive strengths were set as 20 MPa, 40 MPa, 60 MPa and 80 MPa; the jet velocity was set at 280 m/s; and the abrasive density was set at 3000 kg/m³. As the concentration of abrasive increases, the initial kinetic energy of the abrasive jet increases. The initial kinetic energy of the abrasive water jet with different abrasive concentrations is shown in Table 2.

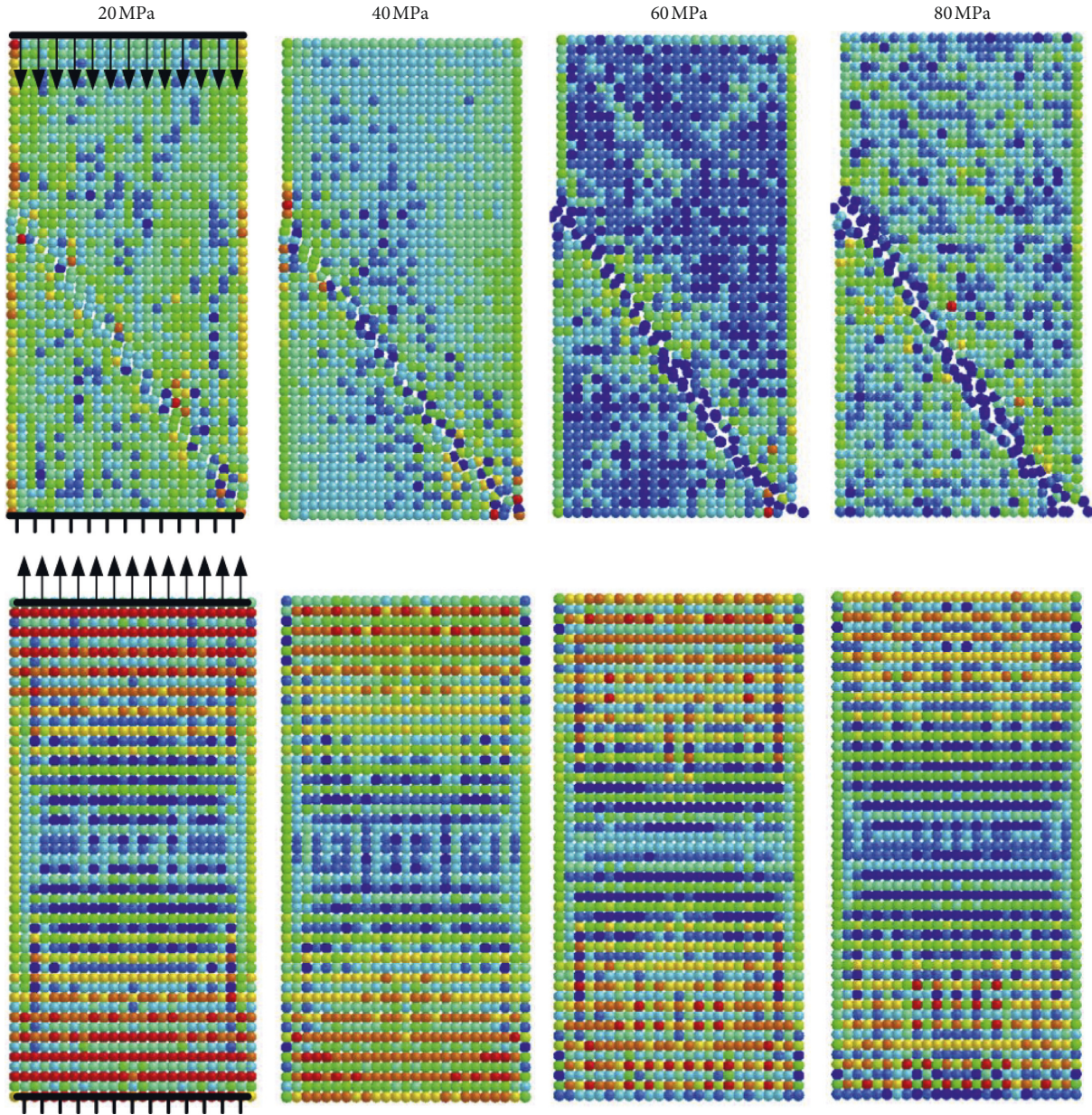


FIGURE 3: Test of compressive and tensile strengths.

TABLE 2: Initial kinetic energy of the abrasive water jet with different abrasive concentrations.

Abrasive concentration (%)	Initial kinetic energy of water (10^{-2} J)	Initial kinetic energy of abrasive (10^{-2} J)	Sum of the initial kinetic energies, E_s (10^{-2} J)
0	6.66	0	6.66
5	6.33	1.0	7.33
10	6.0	2.0	8.0
20	5.33	4.0	9.33
30	4.66	6.0	10.66

3.1.1. Effect on Impact Force. The increase in the initial kinetic energy of the jet will lead to the increase in jet impact force. To study the effect of the abrasive concentrations on the jet impact force under different compressive strengths, the Y direction force of the constrained particles in Figure 2 is extracted as the jet impact force, shown in Figure 4(a). The

effects of abrasive concentrations on the peak and mean of jet impact force under different compressive strengths are shown in Figures 4(b) and 4(c), respectively. The peak of jet impact force is the “water hammer” force generated when the jet is just in contact with concrete, and the mean impact force is the average value of the impact force from $5.2e - 6$ s to $4.0e - 5$ s.

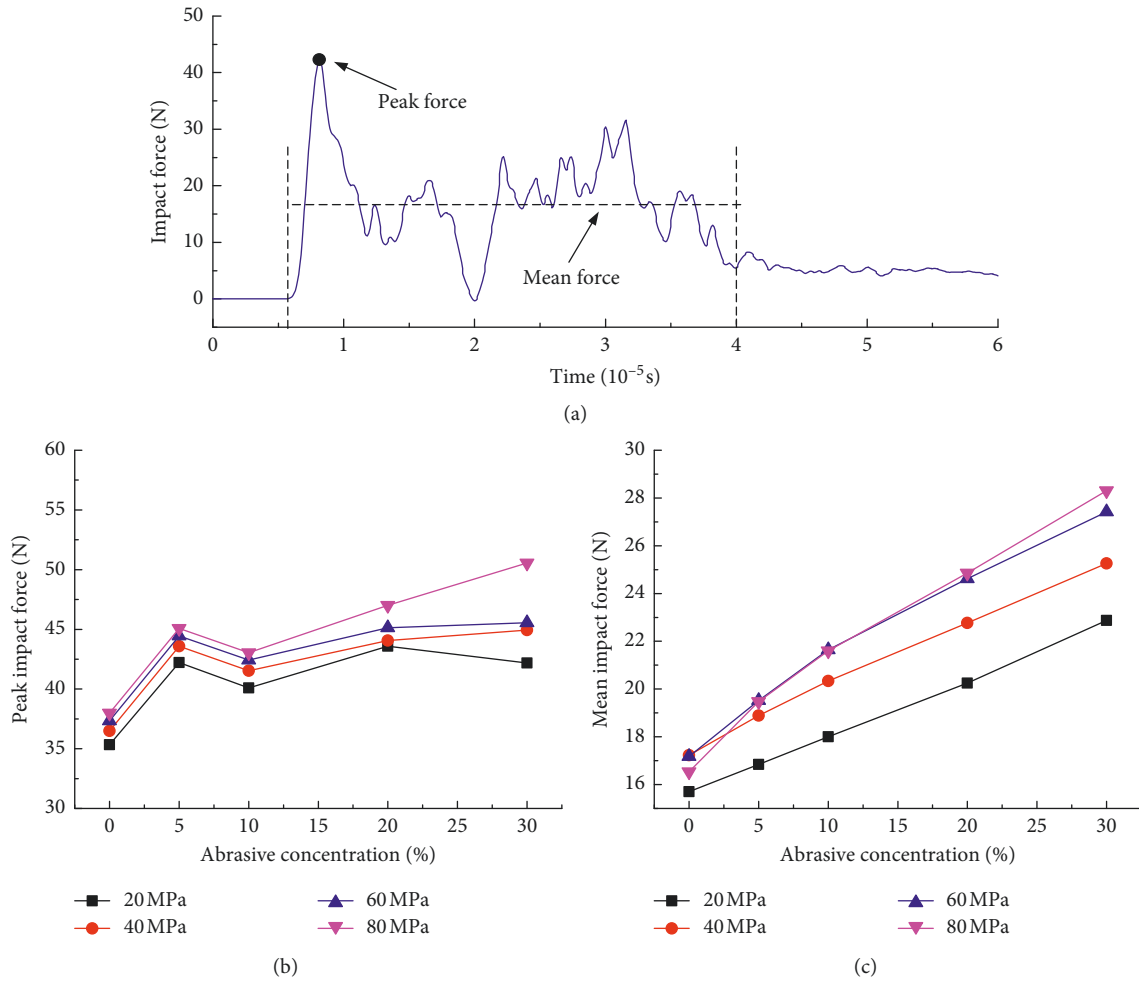


FIGURE 4: Effects of abrasive concentrations on the peak and mean values of jet impact force under different compressive strengths. (a) Impact force (20 MPa, abrasive concentration 5%). (b) Peak of impact force. (c) Mean impact force.

It can be seen from Figure 4(b) that, although the peak impact force of the abrasive jet is significantly improved compared with the pure water jet, the change in the abrasive concentrations under different compressive strengths has little effect on the peak of impact force. Especially for 20~60 MPa, the tested peak of impact force fluctuates between 40 and 45 N. This is mainly related to the number of abrasives first contacting the concrete. From Figure 2, the number of abrasives in the 5%, 10%, 20%, and 30% abrasive jet first contacting the concrete is 4, 2, 8, and 5, respectively. At 20 MPa and 60 MPa, the peak of impact force shows a decreasing trend first and then increasing and decreasing as the abrasive concentration changes from 5% to 30%. Especially at 10% concentration, the peak force is the lowest under different compressive strengths. In addition, the impact force increases with the compressive strength under different abrasive concentrations, which indicates that the impact force is also related to the fracture of concrete. The concrete with high strength is more likely to transmit the impact force continuously, and the crushing of concrete will lead to the discontinuous transmission of the impact force.

From Figure 4(c), it can be observed that the mean impact force under different compressive strengths tends to

increase linearly with the abrasive concentrations and the increasing rate is basically the same. The curves of 60 MPa and 80 MPa have basically coincided, indicating that the mean impact force gradually converges with the increase of compressive strength.

3.1.2. Effect on Internal Energy of Concrete. From the perspective of energy, the process of water jet crushing the concrete material is mainly the process of transforming the kinetic energy of the water jet into the kinetic energy and internal energy of the concrete material. The so-called kinetic energy of the concrete material includes the kinetic energy of the spattered particles, the pressed particles, and the block concrete because of cracks, as shown in Figure 5. Because the kinetic energy of concrete particles was relatively low, corresponding statistical studies was not made.

The internal energy of concrete mainly refers to the deformation energy because of its extrusion, which can characterize the damage to a certain extent. Therefore, it is of great significance to study the internal energy of concrete. Figure 6(a) shows the time history curve of the internal energy of concrete when the compressive strength is 20 MPa

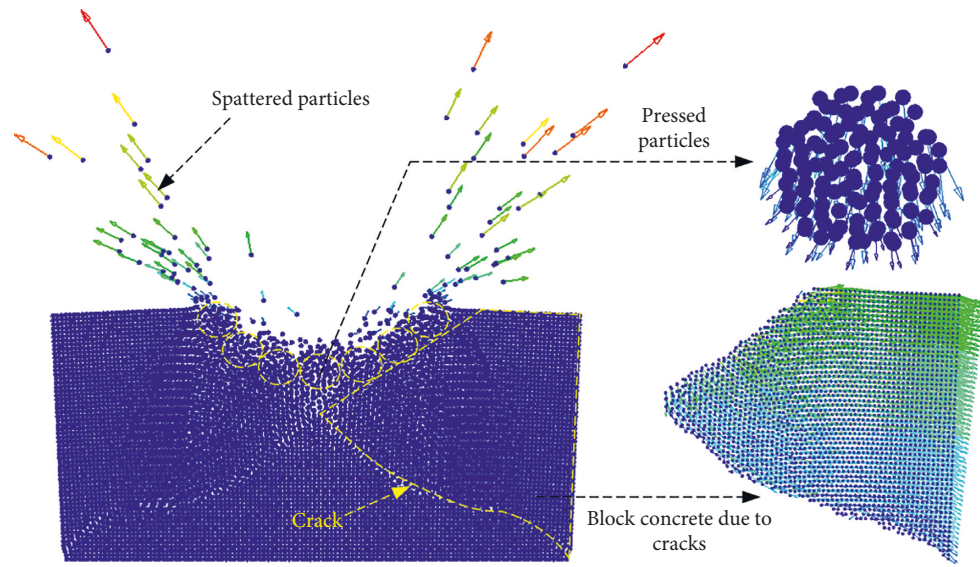


FIGURE 5: Concrete material speed vector (20 MPa, abrasive concentration 20%).

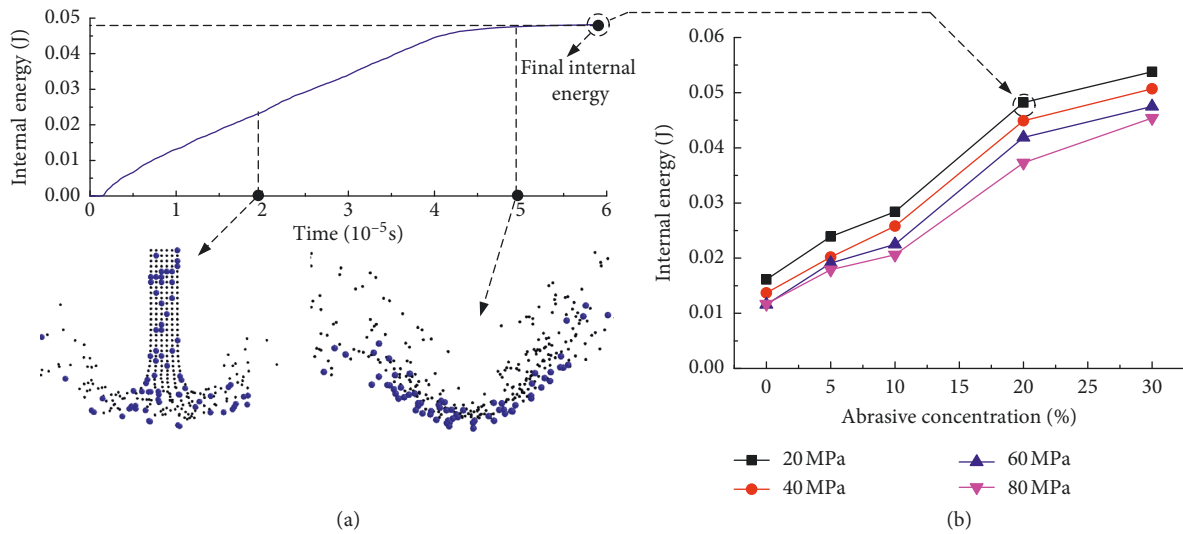


FIGURE 6: (a) Internal energy of 20 MPa with abrasive concentration 20%. (b) Internal energy with different abrasive concentrations.

and the abrasive concentration is 20%. It can be seen that the internal energy of concrete increases linearly in the jet impacting period ($5e-6s \sim 4e-5s$). After $5e-5s$, the jet impacting completes, and the internal energy of concrete remains basically unchanged.

The final internal energy of the concrete was counted, and the effect of the abrasive concentrations on the internal energy of the concrete under different compressive strengths is shown in Figure 6(b). The internal energy of concrete increases stepwise with the abrasive concentrations under different compressive strengths. The so-called stepwise growth trend means that the internal energy of concrete increases by 5% compared with that of the pure water jet, while the growth of 10% is slower than that of 5%, and it increases greatly by 20%, while growth slows again from 20% to 30%. Due to the increase of compressive strength, the damage resistance ability of concrete becomes stronger. The internal energy decreases with

the compressive strength under the same abrasive concentrations, and the decrease amplitudes under different compressive strengths are not much different.

3.1.3. Effect on Crushing Depth and Damage of Concrete. Impact force and concrete internal energy can reflect the impact performance of the abrasive jet to a certain extent, but the purpose of impacting is to make crushing and damage concrete. Thus, crushing and damage of concrete is a more important criterion to measure the impact performance of the abrasive jet. The crushing and damage of concrete under different compressive strengths and abrasive concentrations obtained using numerical simulation are shown in Figure 7.

It can be seen from Figure 7 that the concrete particles splash and extrude to form a crushing pit under the impact

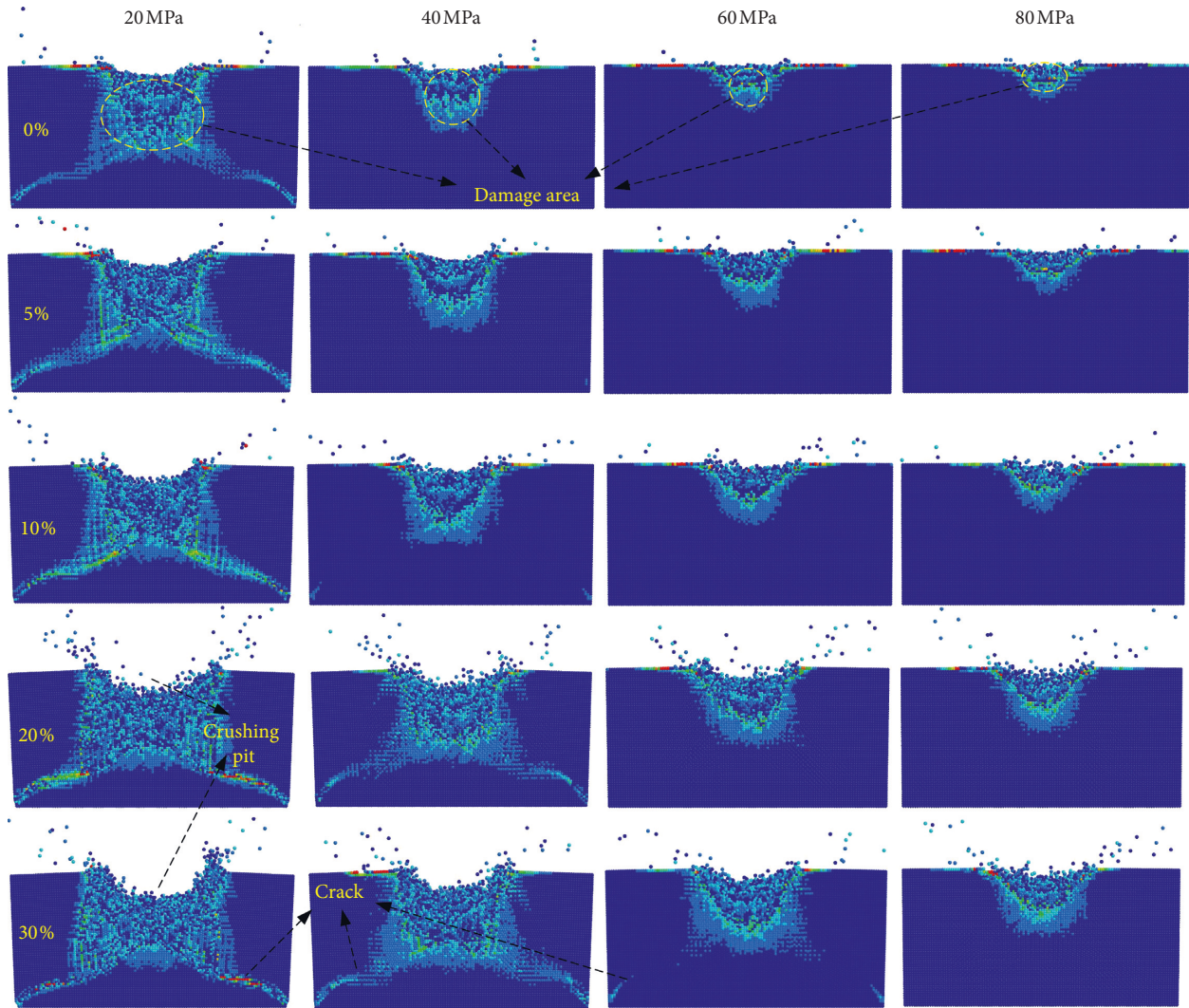


FIGURE 7: Crushing and damage of concrete under different compressive strengths and abrasive concentrations.

of the water jet, and the unbroken part is damaged by the extrusion. The crushing pit and the damage area become larger gradually as the abrasive concentration increases under different compressive strengths. In addition to the crushing pit and damage, there are cracks in the concrete with small compressive strength at the same time, and the cracks become more and more obvious as the abrasive concentration increases.

For this reason, crushing and damage of concrete is a more important criterion to measure the impact performance of the jet, and the quantitative statistics was taken on the crushing depth and damage. The method is shown in Figure 8. The crushing depth is the maximum coordinate of the jet particles in the $-Y$ direction, and the damage area is characterized by the number of particles whose extracted stress values are close to 0.

The effects of the abrasive concentration on the crushing depth and damage under different compressive strengths are shown in Figures 9(a) and 9(b), respectively.

From Figure 9(a), the crushing depth under different compressive strengths shows an increasing trend with the

abrasive concentration, but the change trend is different. For 20 MPa and 40 MPa, the crushing depth changes linearly with the abrasive concentration from 0% to 20%, while the growth rate from 20% to 30% becomes slower. For 60 MPa and 80 MPa, the abrasive water jet has little effect on increasing the crushing depth with abrasive concentration changing from 5% to 10%. The depth increases greatly until the concentration is 20%, and when exceeding 20%, the crushing depth increases slowly or even hardly increases.

From Figure 9(b), the trends of the damage with the abrasive concentration are basically the same under different compressive strengths, and all show a stepwise increasing trend. The so-called stepwise trend is similar to the change in concrete internal energy (Figure 6(b)). It can be seen that the concrete internal energy can indeed reflect the damage to a certain extent. The difference is that the damage decreases with the compressive strength, and the decreasing amplitude increases gradually with the abrasive concentration, which indicates that it is easier to increase the damage by increasing abrasive concentration for the concrete with small compressive strength.

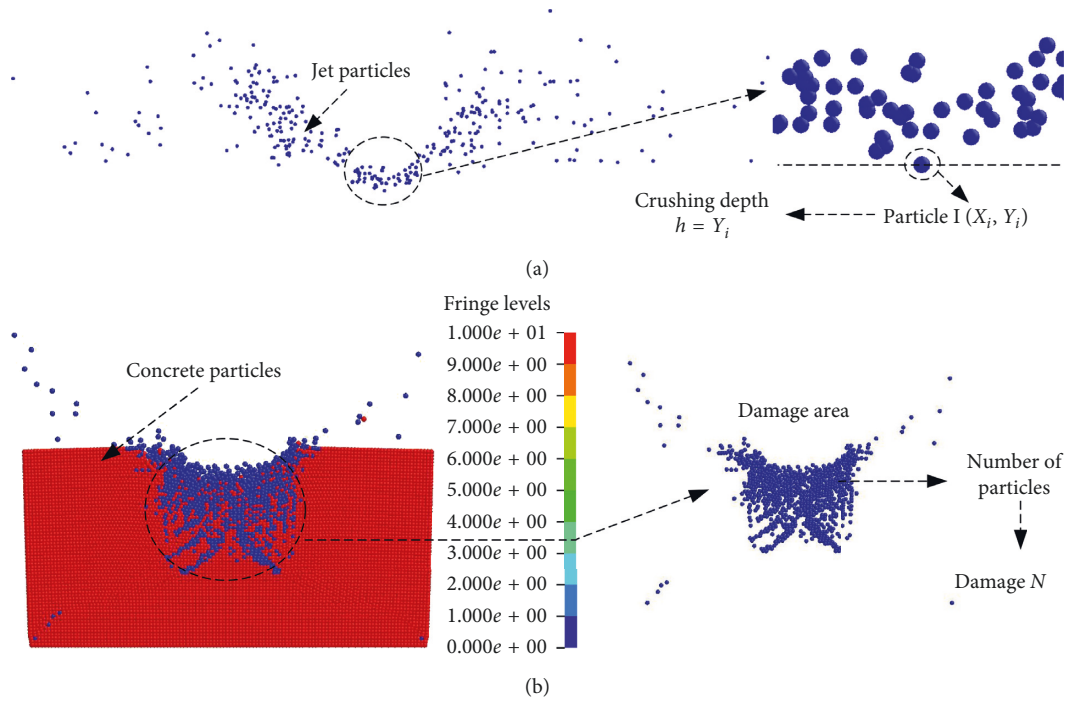


FIGURE 8: Definition of (a) crushing depth and (b) damage.

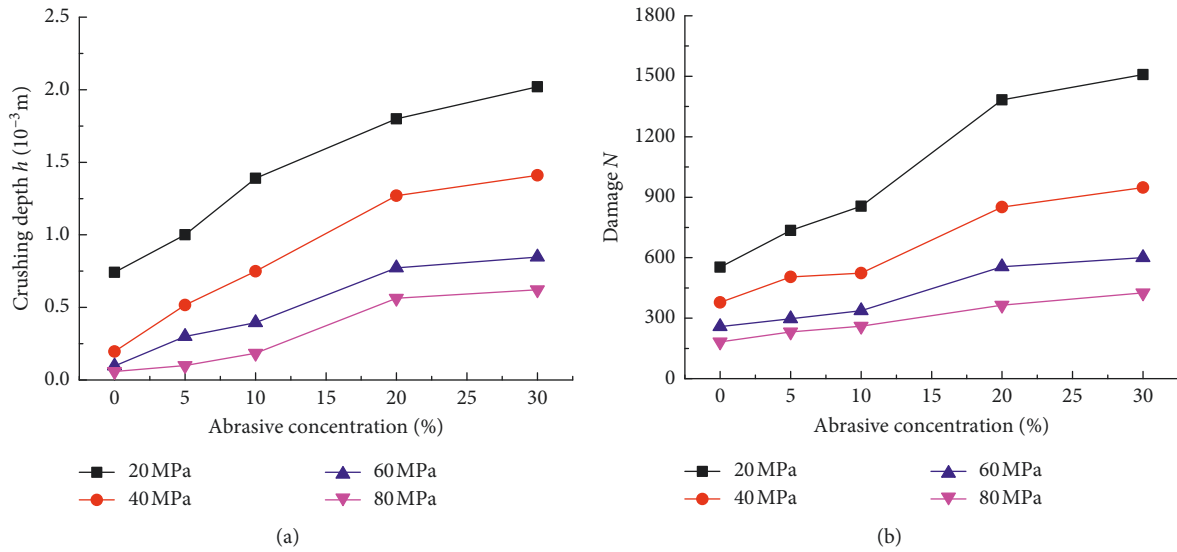


FIGURE 9: Effects of the abrasive concentration on the crushing depth (h) (a) and damage (N) (b) under different compressive strengths.

In order to further analyze the impact performance of the abrasive jet, two indexes of crushing depth efficiency and damage efficiency are introduced, which are the ratio of the crushing depth h and the damage N to the initial kinetic energy of the abrasive jet E_s . The effects of the abrasive concentration on the crushing depth efficiency and damage efficiency under different compressive strengths are shown in Figures 10(a) and 10(b), respectively.

From Figure 10(a), the crushing depth efficiency increases first and then decreases with the abrasive concentration under different compressive strengths and peaks at a concentration of 20%. It means that the crushing depth efficiency will not

increase but decrease when the abrasive concentration exceeds 20%. Compared with the pure water jet, the crushing efficiency increasing rate of the 20% concentration jet increases with the compressive strength, indicating that the abrasive jet is more meaningful to improve crushing depth efficiency of high compressive strength concrete. In addition, although the crushing depth efficiency is the largest when the abrasive concentration is 20% for different compressive strengths, the change trend is different. For example, the difference is not large in crushing depth efficiency between the abrasive concentrations of 10% and 20% for 20 MPa concrete, and the jet with the abrasive concentration of 10% has met the

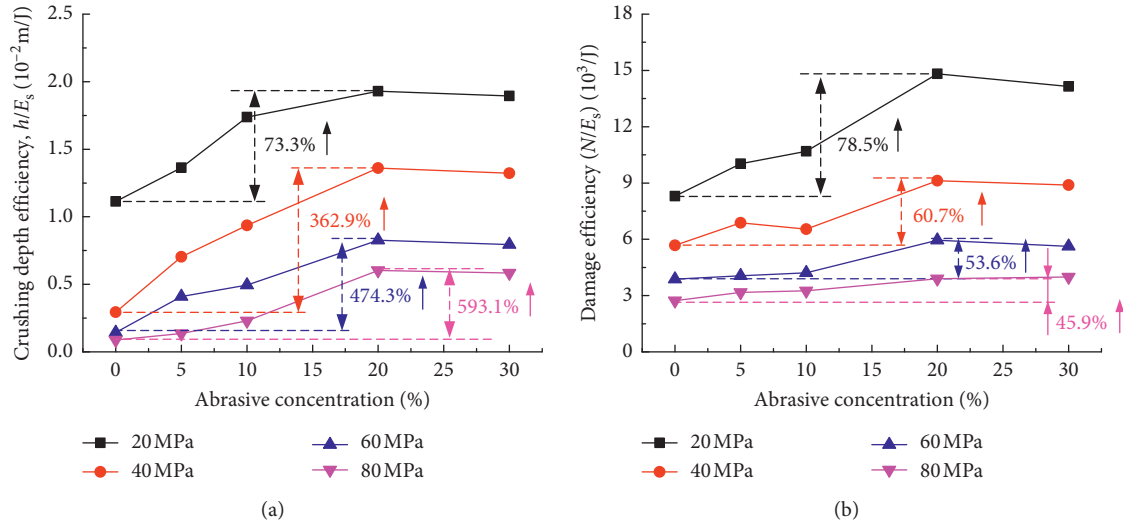


FIGURE 10: Effects of the abrasive concentration on the (a) crushing depth efficiency and (b) damage efficiency under different compressive strengths.

requirements for the crushing depth efficiency. However, for 80 MPa concrete, there is a large difference in crushing depth efficiency between the abrasive concentrations of 10% and 20%. And the concentrations must reach 20% to achieve higher crushing depth efficiency.

From Figure 10(b), the trend of damage efficiency is the same with that of crushing depth efficiency. And it also peaks at the concentration of 20%. Compared with the pure water jet, the damage efficiency increasing rate of the jet with the 20% concentration of abrasive decreases with the compressive strength, indicating that the abrasive jet is more meaningful to improve damage efficiency of low compressive strength concrete. Moreover, the damage efficiency increases slowly with the abrasive concentrations from 0 to 10% under different compressive strengths and shows a rapid increase from 10% to 20%. It can be concluded that it is necessary to use an abrasive jet of concentration of about 20% to greatly improve the damage efficiency.

3.1.4. Effect on Distribution of Abrasive Particles. After the water from the water jet impacted the concrete, it was divided into two parts. One part was the rebounding particles with higher speed, and the other part was the intrusive particles with lower speed. The rebounding particles moved away from the concrete mass at a constant speed after a direct or indirect interaction with the concrete, generally formed by the outer edge of the jet. The intrusive particles were mainly formed by the center of the jet and contributed mainly to the crushing and damage of the concrete. The more the intrusive particles, the more the energy of the concrete directly impacted by the jet, especially the abrasive intrusive particles.

Figure 11 shows the distribution of abrasive particles after a water jet of 20% abrasive concentration impacted 20 MPa concrete. The jet is divided into 6 columns, with columns 1, 2 in the center and columns 5, 6 at the outer edge. Figure 11(a) shows the distribution of all abrasive particles after the impact was completed. It can be seen from

Figures 11(b)–11(d) that the abrasive intrusive particles are mainly formed by columns 1, 2; both intrusive particles and rebounding particles are formed by columns 3, 4; and columns 5, 6 form substantially only rebounding particles.

Figure 12 shows the abrasive particle distribution of water jets with different abrasive concentrations impacting 20 MPa concrete. It can be seen that, as the abrasive concentration increases, the intrusive particles almost increase proportionally, which effectively explains the increasing trend of the crushing depth and damage.

However, from Figure 10, the proportional increase of intrusive particles does not make the crushing depth and damage increase proportionally. It means that the crushing depth and damage has shown a slow growth trend, especially for that of the 10% concentration relative to the 5% concentration and that of the 30% concentration relative to the 20% concentration. The main reason is that the particles accumulation occurs so that the impact energy is buffered and consumed, and the due crushing and damage effects are not achieved. From Figure 12, the accumulation of intrusive particles is serious in Figures 12(c) and 12(e) compared with that in Figures 12(b) and 12(d). It indicates that the intrusive particles that are in contact with the concrete first form a water cushion before the impact of the later particles. When impacting, the later particles is actually in direct contact with the previous intrusive particles, rather than the concrete, so that the early particles have a buffering effect on the impact of the later particles, and the crushing and damage effects are not achieved that of the direct impact.

Figure 13 shows the abrasive particle distribution of different compressive strength concrete impacted by using the water jet with 20% abrasive concentration. As the compressive strength of the concrete increases, the depth of the jet particles intruding into the concrete decreases gradually. When the depth becomes smaller, the abrasive particles surrounded by the concrete crushing pit become less, which results in larger rebounding angle and more rebounding abrasive particles. The more the rebounding

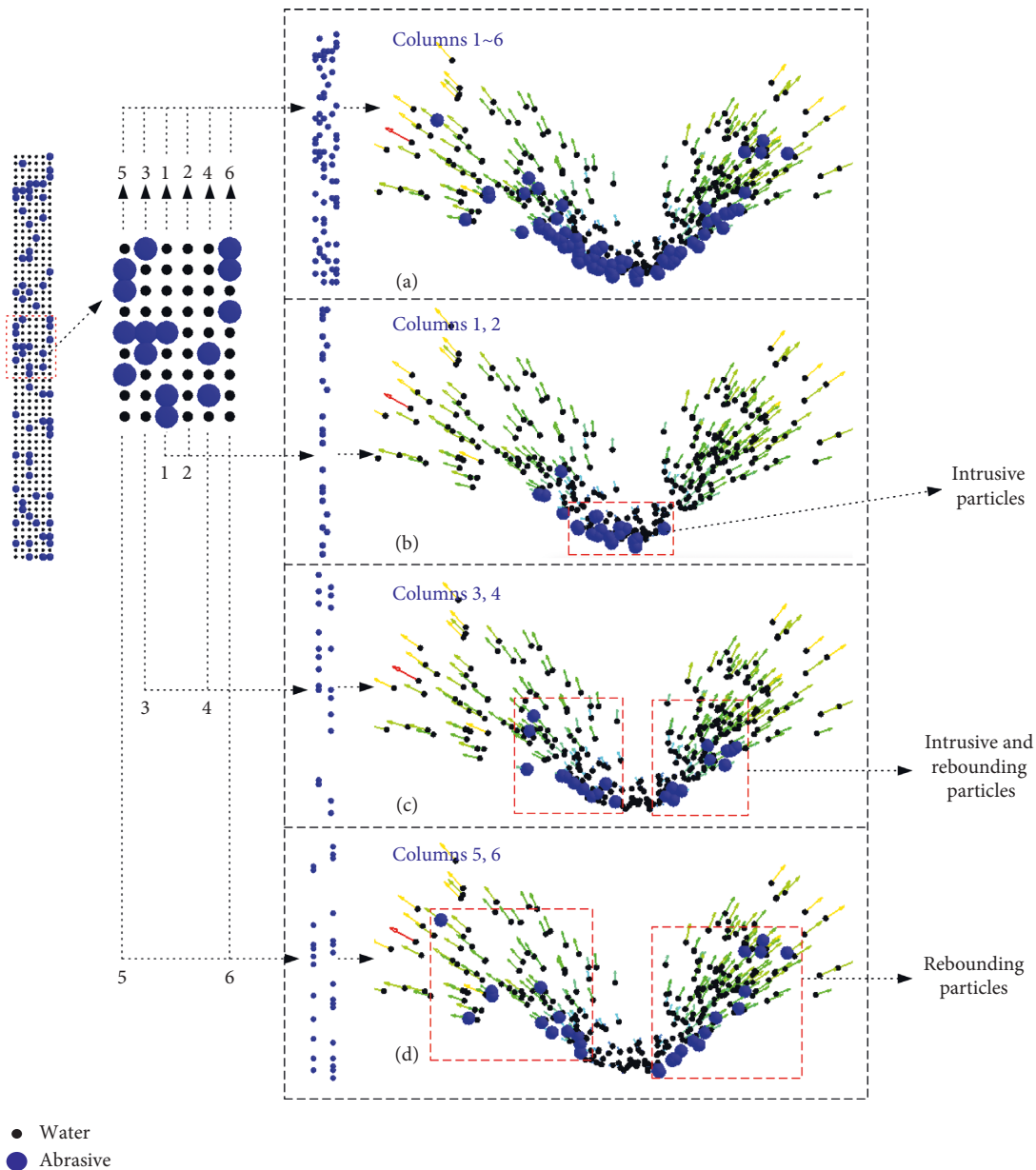


FIGURE 11: Distribution of abrasive particles (20 MPa, abrasive concentration 20%).

abrasive particles, the less the intrusive abrasive particles. And the depth will be further smaller.

3.2. Effect of Abrasive Concentration under Different Abrasive Densities. To study the effect of abrasive concentration on impact performance of the abrasive water jet under different abrasive densities, the abrasive densities were set as 2000 kg/m³, 3000 kg/m³, 4000 kg/m³, and 5000 kg/m³; the concrete compressive strength was set at 40 MPa; the jet velocity was still set at 280 m/s. The initial kinetic energy of the water jet with different abrasive concentrations is shown in Table 3.

3.2.1. Effect on Impact Force. The increase in abrasive density and the abrasive concentration increase the initial kinetic energy of the jet, which leads to the increase of jet

impact force at the same time. The effects of abrasive concentration on the peak and mean of jet impact force under different abrasive densities are shown in Figures 14(a) and 14(b), respectively. The statistical method of peak and mean of impact force is the same as in Figure 4.

It can be seen from Figure 14(a) that the change of the abrasive concentration under different abrasive densities has little effect on the peak of impact force. Especially for the jet of abrasive density 2000 kg/m³, the tested peak of impact force fluctuates around 40 N. And there is a small increasing trend under the other densities. The drop in 10% concentration is also related to the number of abrasives first contacting with the concrete. Under the same abrasive concentration, the peak force basically increases uniformly with the abrasive density, but the larger the concentration, the greater the increase.

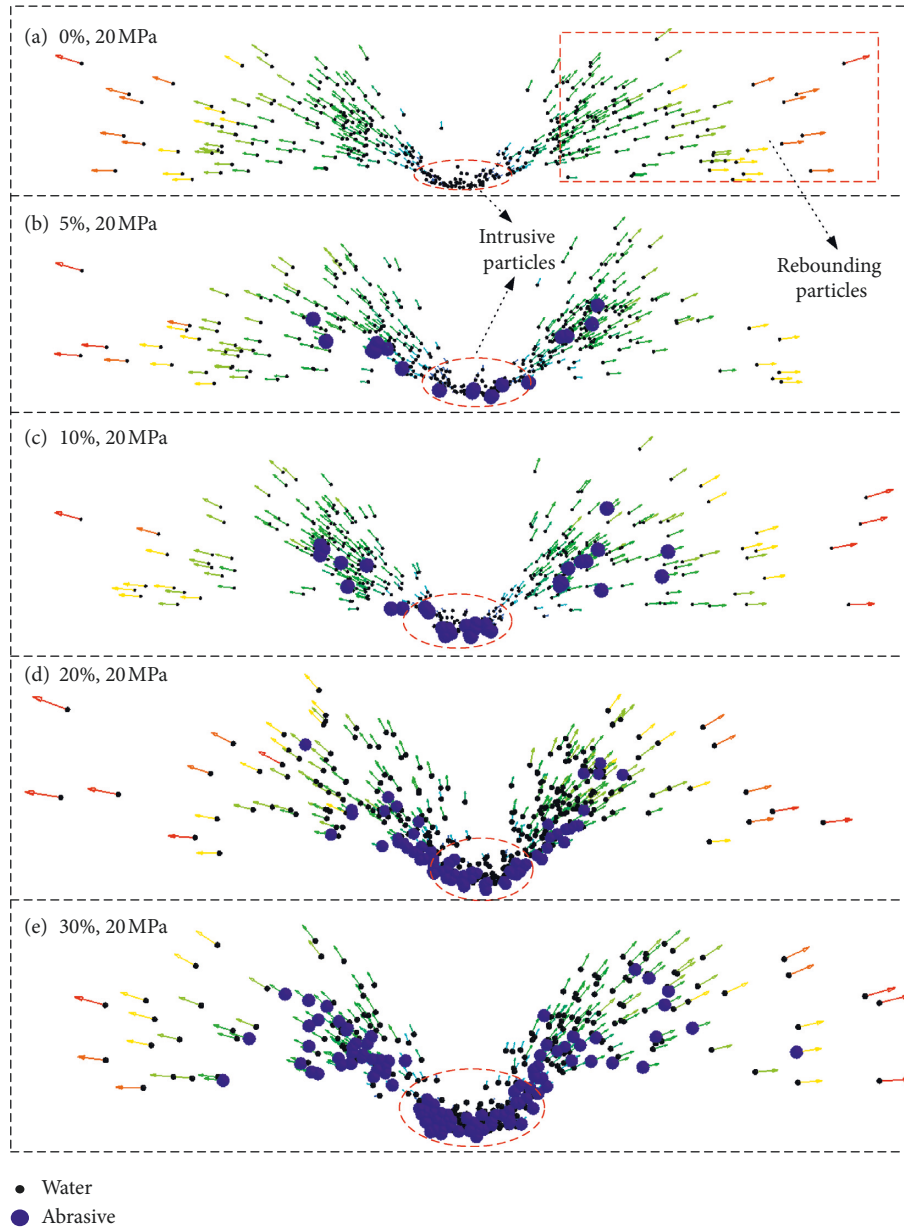


FIGURE 12: Abrasive particle distribution of water jets with different abrasive concentrations impacting 20 MPa concrete.

From Figure 14(b), the mean impact force increases linearly with the abrasive concentration under different abrasive densities. The larger the abrasive density, the greater the increase. Under the same abrasive concentration, same with the peak force in trend, the mean force basically increases uniformly with the abrasive density, and the larger the concentration, the greater the increase.

3.2.2. Effect on Internal Energy of Concrete. Figure 15 shows the effect of the abrasive concentration on the internal energy of the concrete under different abrasive densities. Under different abrasive densities, the internal energy of concrete increases stepwise with the abrasive concentration. 10%~20% is the rapid increasing stage, and the larger the abrasive density, the greater the increase; while 5%~10% and 20%~30% are the slow increasing stages, and the increase of

different abrasive densities is not much different. Under the same abrasive concentration, the internal energy of the concrete increases uniformly with the abrasive density, and the larger the concentration, the greater the increase.

3.2.3. Effect on Crushing Depth and Damage of Concrete.

Figure 16 shows the crushing and damage of concrete under different abrasive concentrations and densities. The quantitative statistics was also taken on the crushing depth and damage. And the effects of the abrasive concentration on the crushing depth and damage under different abrasive densities are shown in Figures 16(b) and 16(c), respectively.

From Figure 16, the crushing pit and the damage area become larger gradually as the abrasive concentration and density increase. And the trends of concrete crushing depth and damage with concentration are basically consistent with

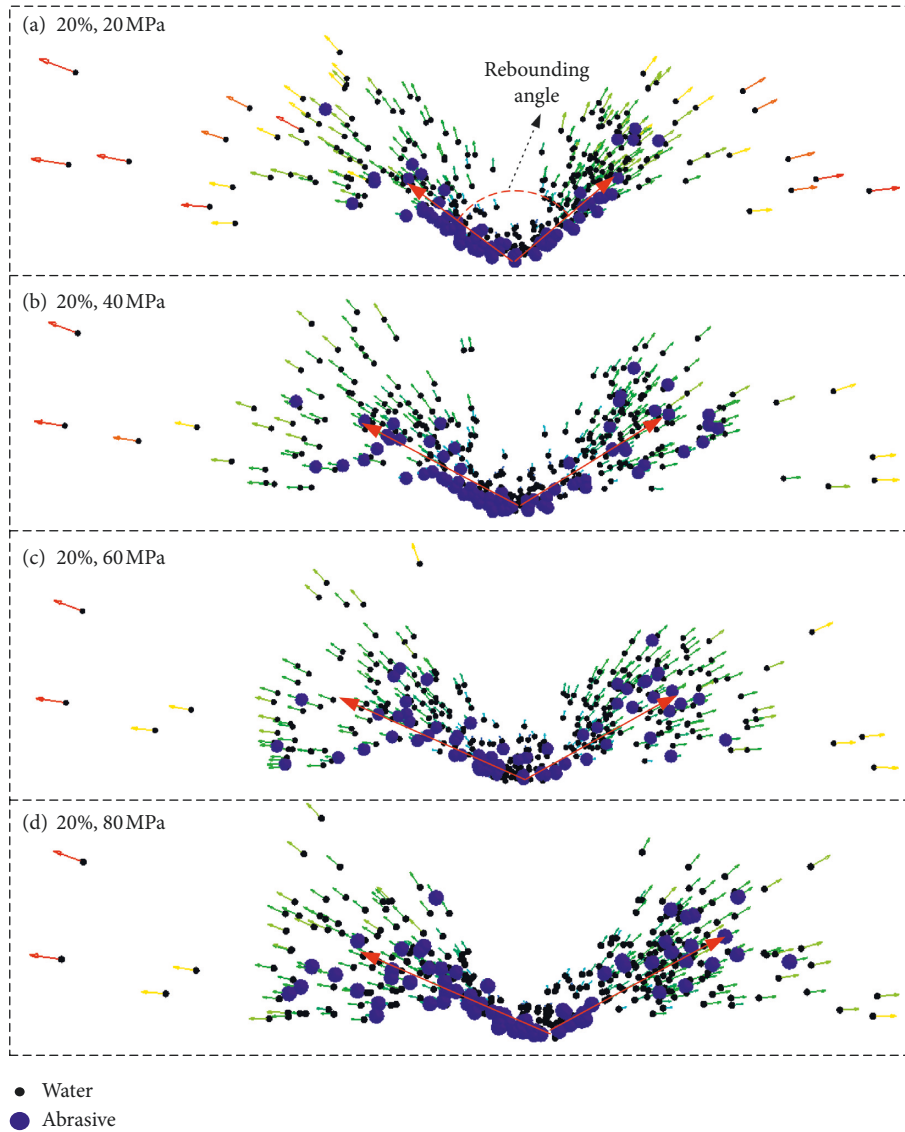


FIGURE 13: Abrasive particle distribution of different compressive strength concrete impacted by using the water jet with 20% abrasive concentration.

TABLE 3: Initial kinetic energies of the water jet with different abrasive concentrations and densities.

Abrasive density (kg/m^3)	Initial kinetic energy of 5% concentration, E_s (10^{-2} J)	Initial kinetic energy of 10% concentration, E_s (10^{-2} J)	Initial kinetic energy of 20% concentration, E_s (10^{-2} J)	Initial kinetic energy of 30% concentration, E_s (10^{-2} J)
2000	7.00	7.33	7.99	8.66
3000	7.33	8.00	9.33	10.66
4000	7.66	8.66	10.66	12.66
5000	8.00	9.33	11.99	14.66

the trend of internal energy, and both are in a stepwise increasing trend. 10%~20% is still the rapid increasing stage, and the larger the abrasive density, the greater the increase. It can be proved again that the concrete internal energy can reflect the damage to some extent.

Similarly, to further analyze the impact performance of the jet, crushing depth efficiency and damage efficiency are introduced. The effects of the abrasive concentration on the

crushing depth efficiency and damage efficiency under different abrasive densities are shown in Figures 17(a) and 17(b), respectively.

From Figure 17, firstly, the crushing depth efficiency and the damage efficiency are both maximum when the abrasive concentration is 20% under different abrasive densities, and the efficiency increase is not obvious or even decreases greatly when the concentration is higher than 20%; secondly,

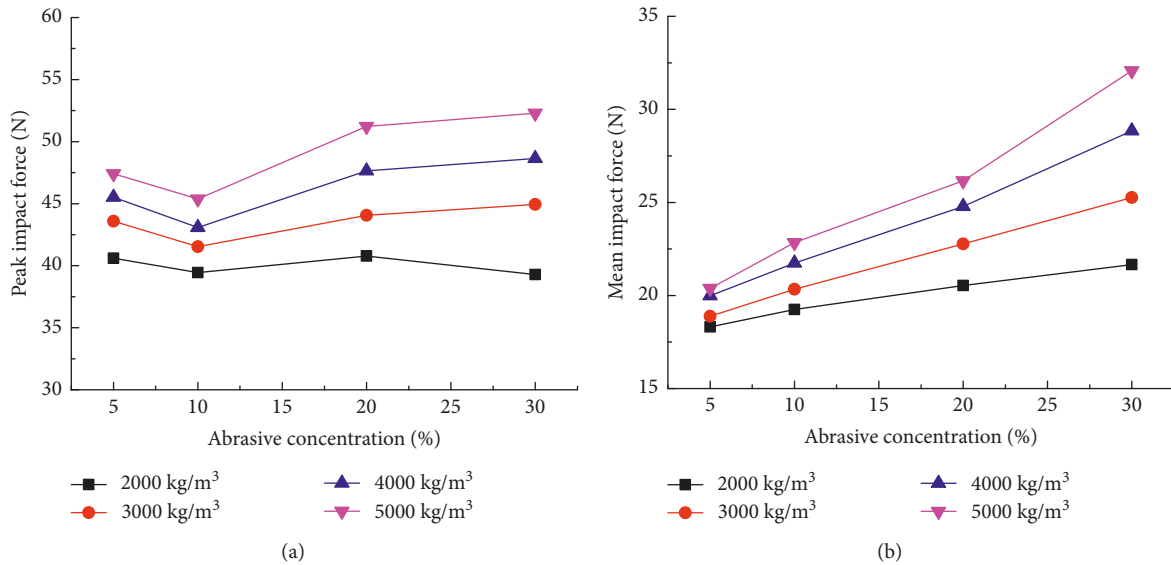


FIGURE 14: Effects of abrasive concentration on the peak (a) and mean (b) of jet impact force under different abrasive densities.

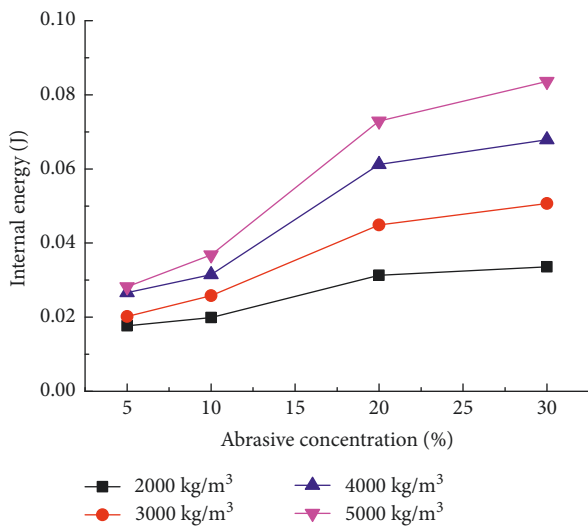


FIGURE 15: Effect of the abrasive concentration on the internal energy of the concrete under different abrasive densities.

the efficiency of concentration of 10% is not much different from that of concentration of 5%, which even has a downward trend; thirdly, the crushing depth efficiency and damage efficiency of concentration of 20% and density of 2000 kg/m³ are higher than those of concentrations of 5% and 10% under all abrasive densities.

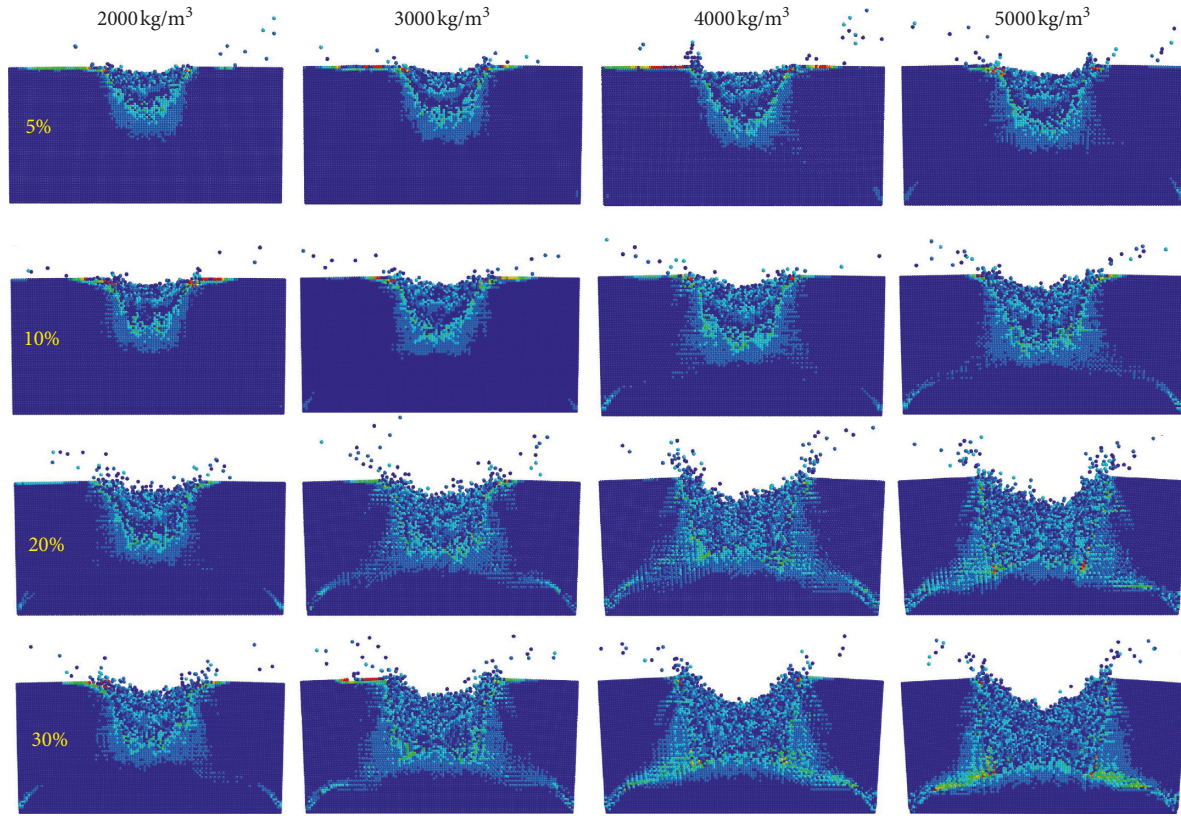
3.2.4. Effect on Distribution of Abrasive Particles. The abrasive particle distribution of abrasive jets with different abrasive concentrations impacting concrete has been given above and will not be studied again. Figure 18 shows the abrasive particle distribution of the abrasive jets with different abrasive densities impacting concrete.

As the abrasive density increases, the depth of the jet particles intruding into the concrete increases gradually.

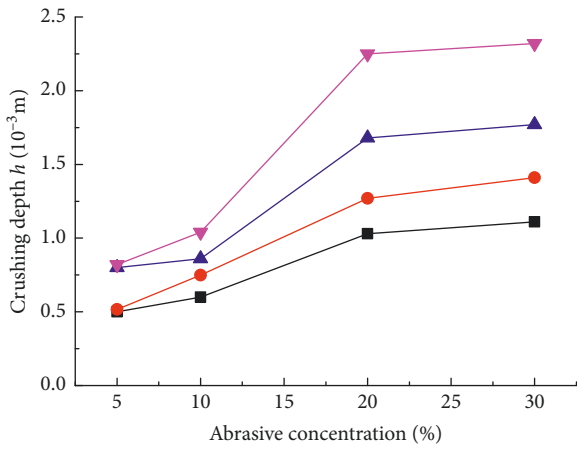
When the depth becomes larger, the abrasive particles surrounded by the concrete crushing pit become more, which results in smaller rebounding angle and less rebounding abrasive particles. The less the rebounding abrasive particles, the more the intrusive abrasive particles. And the depth will be further larger. Moreover, the depth is continuously deepened so that the intrusive particles can continuously intrude downward, which reduces the accumulation of abrasive particles and then the impact energy loss, and improves the impact efficiency.

4. Conclusions

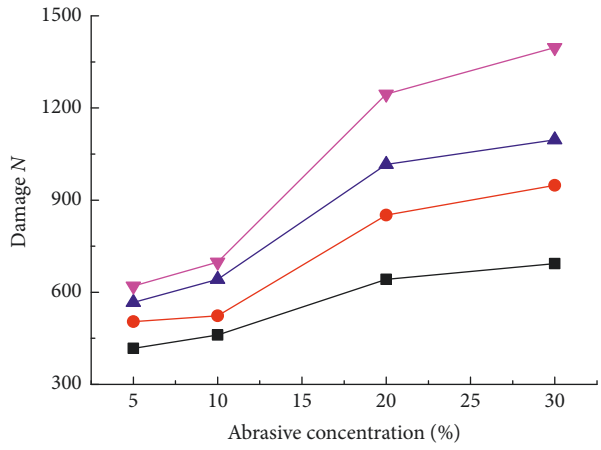
- (1) There is little effect of the abrasive concentration on the peak impact force under different compressive strengths and abrasive densities, while the mean impact force tends to increase linearly with the abrasive concentration. The mean impact force gradually converges with the increase of compressive strength and basically increases uniformly with the abrasive density.
- (2) The internal energy of concrete increases stepwise with the abrasive concentrations under different compressive strengths and abrasive densities. Concentration of 10%~20% is the rapid increasing stage. Under the same abrasive concentration, the internal energy of the concrete decreases with the compressive strength, and the decrease in amplitude under different compressive strengths is not much different; while the internal energy increases uniformly with the abrasive density, and the larger the concentration, the greater the increase. Moreover, it has been proved that the internal energy can reflect the damage to some extent.
- (3) The crushing depth efficiency and damage efficiency are both maximum at a concentration of 20% under



(a)



(b)



(c)

FIGURE 16: (a) Crushing and damage of concrete and quantitative statistics: (b) crushing depth (h) and (c) damage (N), under different abrasive concentrations and densities.

different compressive strengths. The crushing depth efficiency of concentration of 10% has almost achieved that of concentration of 20% for small compressive strength concrete (20 MPa), while the concentration must reach 20% to achieve higher crushing efficiency for great compressive strength concrete (80 MPa). In contrast, it is necessary to use

an abrasive jet of concentration of about 20% to greatly improve the damage efficiency.

Compared with the pure water jet, the crushing depth efficiency and damage efficiency increasing rate of the 20% concentration jet increases and decreases with the compressive strength, respectively, indicating that the abrasive jet is more meaningful to

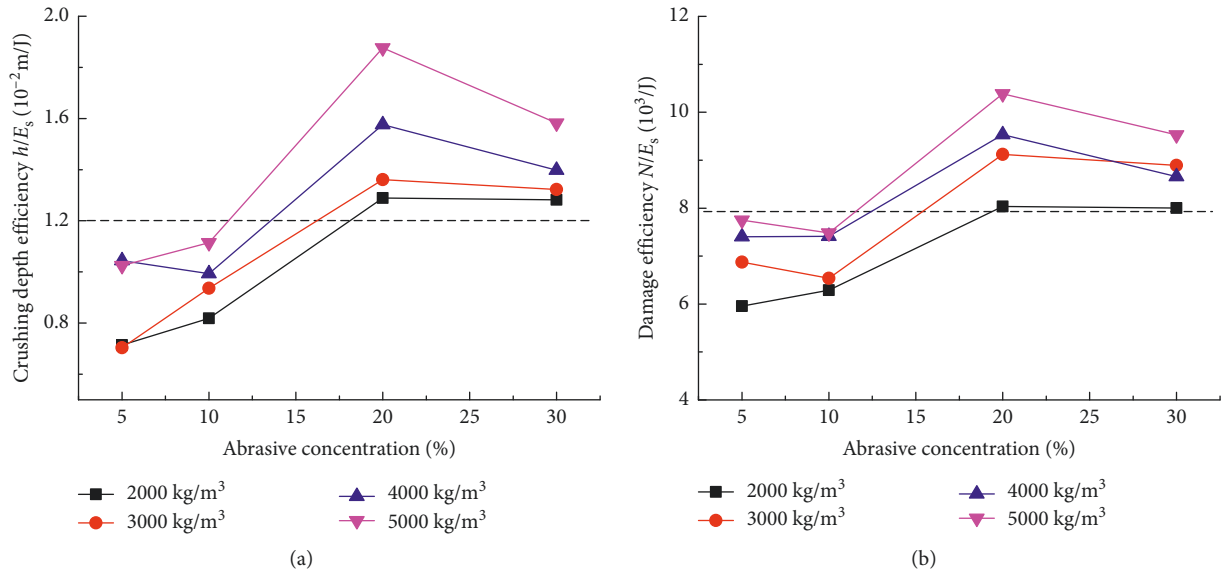


FIGURE 17: Effects of the abrasive concentration on the crushing depth efficiency (a) and damage efficiency (b) under different abrasive densities.

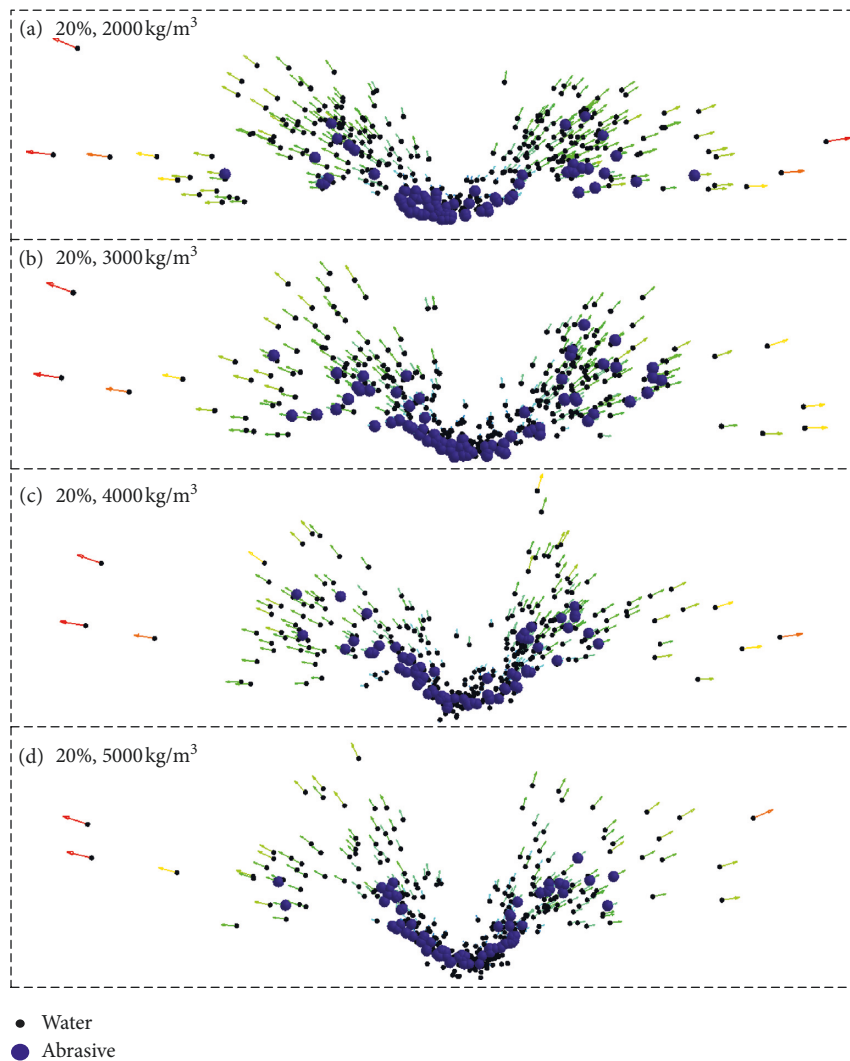


FIGURE 18: Abrasive particle distribution of the abrasive jets with different abrasive densities impacting concrete.

improve crushing depth efficiency of high compressive strength concrete and damage efficiency of low compressive strength concrete.

The crushing depth efficiency and the damage efficiency are both maximum when the abrasive concentration is 20% under different abrasive densities, and the efficiency increase is not obvious or even decreases greatly when the concentration is higher than 20%. The efficiencies of concentration of 10% is not much different from that of concentration of 5% and even has a downward trend. The efficiencies of concentration of 20% and density of 2000 kg/m³ are higher than those of concentrations of 5% and 10% under all abrasive densities.

The conclusion that most efficient concentration is 20% can be verified by the experiment in reference [31], in which the effect of abrasive concentration on damaged volume rate was studied, and the maximum value is at a concentration of about 20%.

- (4) After the water from the water jet impacted the concrete, it was divided into two parts. One part was the rebounding particles with higher speed formed by the outer edge of the jet, and the other part was the intrusive particles with lower speed formed by the center of the jet. The more the intrusive particles, the easier the concrete to be crushed and damaged.

The intrusive particles almost increase proportionally with the abrasive concentration, which effectively explains the increasing trend of the crushing depth and damage. However, the proportional increase of intrusive particles does not make the crushing depth and damage increase proportionally, which is because of the particle's accumulation so that the impact energy is buffered and consumed, and the due crushing and damage effects are not achieved.

The intrusive abrasive particle increases with the abrasive density and decreases with the compressive strength. The more the intrusive abrasive particle, the greater the crushing depth. The intrusive particles can continuously intrude downward with the depth continuously deepened, which reduces the accumulation of abrasive particles and then the impact energy loss and improves the impact efficiency.

Data Availability

The data used to support the findings of this study are available from the corresponding author upon request.

Conflicts of Interest

The authors declare that they have no conflicts of interest.

Acknowledgments

This project was supported by the National Natural Science Foundation of China (51705029) and the Fundamental Research Funds for the Central Universities (300102258302 and 300102258101).

References

- [1] X. Liu, S. Liu, and H. Ji, "Numerical research on rock breaking performance of water jet based on SPH," *Powder Technology*, vol. 286, pp. 181–192, 2015.
- [2] Y. Ozcelik, A. E. Tercan, E. Yilmazkaya, R. Ciccu, and G. Costa, "A study of nozzle angle in stone surface treatment with water jets," *Construction and Building Materials*, vol. 25, no. 11, pp. 4271–4278, 2011.
- [3] Y. Ozcelik, R. Ciccu, and G. Costa, "Comparison of the water jet and some traditional stone surface treatment methods in different lithotypes," *Construction and Building Materials*, vol. 25, no. 2, pp. 678–687, 2011.
- [4] S. Dehkhoda and M. Hood, "An experimental study of surface and sub-surface damage in pulsed water-jet breakage of rocks," *International Journal of Rock Mechanics and Mining Sciences*, vol. 63, pp. 138–147, 2013.
- [5] S. Dehkhoda and M. Hood, "The internal failure of rock samples subjected to pulsed water jet impacts," *International Journal of Rock Mechanics and Mining Sciences*, vol. 66, pp. 91–96, 2014.
- [6] X. Yang, X. Li, and Y. Lu, "Wear characteristics of the cemented carbide blades in drilling limestone with water jet," *International Journal of Refractory Metals and Hard Materials*, vol. 29, no. 2, pp. 320–325, 2011.
- [7] R. Ciccu and B. Grosso, "Improvement of disc cutter performance by water jet assistance," *Rock Mechanics and Rock Engineering*, vol. 47, no. 2, pp. 733–744, 2014.
- [8] R. Ciccu and B. Grosso, "Improvement of the excavation performance of PCD drag tools by water jet assistance," *Rock Mechanics and Rock Engineering*, vol. 43, no. 4, pp. 465–474, 2010.
- [9] S. Liu, J. Chen, and X. Liu, "Rock breaking by conical pick assisted with high pressure water jet," *Advances in Mechanical Engineering*, vol. 6, article 868041, 2014.
- [10] S. Liu, Z. Liu, X. Cui, and H. Jiang, "Rock breaking of conical cutter with assistance of front and rear water jet," *Tunnelling and Underground Space Technology*, vol. 42, pp. 78–86, 2014.
- [11] X. Liu, S. Liu, and H. Ji, "Mechanism of rock breaking by pick assisted with water jet of different modes," *Journal of Mechanical Science and Technology*, vol. 29, no. 11, pp. 5359–5368, 2015.
- [12] S. Liu, X. Liu, J. Chen, and M. Lin, "Rock breaking performance of a pick assisted by high-pressure water jet under different configuration modes," *Chinese Journal of Mechanical Engineering*, vol. 28, no. 3, pp. 607–617, 2015.
- [13] X. Liu, S. Liu, L. Li, and X. Cui, "Experiment on conical pick cutting rock material assisted with front and rear water jet," *Advances in Materials Science and Engineering*, vol. 2015, Article ID 506579, 9 pages, 2015.
- [14] R. Gryc, L. M. Hlaváč, M. Mikoláš, J. Šancer, and T. Daněk, "Correlation of pure and abrasive water jet cutting of rocks," *International Journal of Rock Mechanics and Mining Sciences*, vol. 65, pp. 149–152, 2014.
- [15] R. Selvam, L. Karunamoorthy, and N. Arunkumar, "Investigation on performance of abrasive water jet in machining hybrid composites," *Materials and Manufacturing Processes*, vol. 32, no. 6, pp. 700–706, 2016.
- [16] M. I. Wong, A. Azmi, C. Lee, and A. Mansor, "Kerf taper and delamination damage minimization of FRP hybrid composites under abrasive water-jet machining," *International Journal of Advanced Manufacturing Technology*, vol. 94, no. 5–8, pp. 1727–1744, 2018.

- [17] H. Liu, J. Wang, R. Brown, and N. Kelson, "Computational fluid dynamics (CFD) simulation of ultrahigh velocity abrasive waterjet," *Key Engineering Materials*, vol. 233–236, no. 1, pp. 477–482, 2003.
- [18] H. Liu, J. Wang, N. Kelson, and R. J. Brown, "A study of abrasive waterjet characteristics by CFD simulation," *Journal of Materials Processing Technology*, vol. 153–154, no. 1, pp. 488–493, 2004.
- [19] G. Hu, W. Zhu, T. Yu, and J. Yuan, "Numerical simulation and experimental study of liquid-solid two-phase flow in nozzle of DIA jet," *Communications in Computer and Information Science*, vol. 15, pp. 92–100, 2008.
- [20] J. Meng, Q. Wei, and Y. Ma, "Numerical simulation study on the flow field out of a submerged abrasive water jet nozzle," *Mathematical and Computational Applications*, vol. 21, no. 1, p. 2, 2016.
- [21] D. Deepak, A. Jodel, Cornelio, M. Midhun Abraham, and U. Shiva Prasad, "Numerical analysis of the effect of nozzle geometry on flow parameters in abrasive water jet machines," *Pertanika Journal of Science and Technology*, vol. 25, no. 2, pp. 497–506, 2017.
- [22] W. Gong, J. Wang, and G. Na, "Numerical simulation for abrasive water jet machining based on ALE algorithm," *International Journal of Advanced Manufacturing Technology*, vol. 53, no. 1–4, pp. 247–253, 2011.
- [23] H. Shahverdi, M. Zohoor, and S. Mousavi, "Numerical simulation of abrasive water jet cutting process using the SPH and ALE methods," *International Journal of Advanced Design and Manufacturing Technology*, vol. 5, no. 1, pp. 43–50, 2011.
- [24] H. Jiang, Z. Liu, and K. Gao, "Numerical simulation on rock fragmentation by discontinuous water-jet using coupled SPH/FEA method," *Powder Technology*, vol. 312, pp. 248–259, 2017.
- [25] Y. Feng, J. Wang, and F. Liu, "Numerical simulation of single particle acceleration process by SPH coupled FEM for abrasive water-jet cutting," *International Journal of Advanced Manufacturing Technology*, vol. 59, no. 1–4, pp. 193–200, 2011.
- [26] J. Wang, N. Gao, and W. Gong, "Abrasive waterjet machining simulation by SPH method," *International Journal of Advanced Manufacturing Technology*, vol. 50, no. 1–4, pp. 227–234, 2010.
- [27] L. Guo, S. Deng, and X. Yang, "Numerical simulation of abrasive water jet cutting chemical pipeline based on SPH coupled FEM," *Chemical Engineering Transaction*, vol. 51, pp. 73–78, 2016.
- [28] Y. Xue, H. Si, D. Xu, and Z. Yang, "Experiments on the microscopic damage of coal induced by pure water jets and abrasive water jets," *Powder Technology*, vol. 332, pp. 139–149, 2018.
- [29] J. Li, Z. Qiao, Z. Yang, and X. Zhang, "Influence of abrasive concentration on processing quality of abrasive flow in mesoscopic scale," *Journal of Jilin University*, vol. 47, no. 3, pp. 837–843, 2017.
- [30] C. Mu and L. Rong, "Numerical simulation of damage mechanism of abrasive water jet impaction on rock," *Rock and Soil Mechanics*, vol. 35, no. 5, pp. 1475–1481, 2014.
- [31] W. Xiang, X. Li, Y. Lu, and F. Liang, "The research of the characteristic of rock broken by abrasive water jet," *Chinese Journal of Underground Space Engineering*, vol. 2, no. 1, pp. 170–174, 2006.



Hindawi

Submit your manuscripts at
www.hindawi.com

